IOP Publishing Smart Materials and Structures
Smart Mater. Struct. **26** (2017) 103001 (18pp) https://doi.org/10.1088/1361-665X/aa8347

Topical Review

Review of magnetostrictive vibration energy harvesters

Zhangxian Deng and Marcelo J Dapino

NSF I/UCRC Smart Vehicle Concepts Center, Department of Mechanical and Aerospace Engineering, The Ohio State University, Columbus, OH 43210, United States of America

E-mail: dapino.1@osu.edu

Received 30 March 2017, revised 4 July 2017
Accepted for publication 1 August 2017
Published 7 September 2017

Abstract

The field of energy harvesting has grown concurrently with the rapid development of portable and wireless electronics in which reliable and long-lasting power sources are required. Electrochemical batteries have a limited lifespan and require periodic recharging. In contrast, vibration energy harvesters can supply uninterrupted power by scavenging useful electrical energy from ambient structural vibrations. This article reviews the current state of vibration energy harvesters based on magnetostrictive materials, especially Terfenol-D and Galfenol. Existing magnetostrictive harvester designs are compared in terms of various performance metrics. Advanced techniques that can reduce device size and improve performance are presented. Models for magnetostrictive devices are summarized to guide future harvester designs.

Keywords: magnetostrictive materials, energy harvester, modeling, design

(Some figures may appear in colour only in the online journal)

1. Introduction

The development of wireless and wearable devices has been growing rapidly in the past few decades. The advances in the field have made it possible to reduce the power requirement of common wireless sensor networks to only tens of milliwatts [1]. At those power levels, electrochemical batteries, which are able to provide an energy density of several hundreds of mW h cm^{-3}, are limited to short-term operation due to the volume limitation of wireless and wearable devices. For long-term operation, batteries require recharging or even replacement, while being susceptible to degradation over time due to the memory effect.

The key technologies behind portable and wearable devices, including the central processing unit, the random-access memory, and the hard disk drive, have experienced rapid improvement in accordance to Moore's law [2], as shown in figure 1. However, advances in battery research in terms of energy storage density have substantially lagged behind other electronics. Energy harvesters that can extract electrical power from ambient sources can supplement and, in some cases, replace batteries.

Potential energy harvesting sources include solar, thermal, electromagnetic, and structural vibrations. Solar energy can be directly converted to electrical energy via the photoelectric effect. For a typical cloudless day in summer and for zero zenith angle, the available power density (PD) on the surface of the Earth is about 1.0 W cm^{-2}, where up to 46% can be converted to electrical energy using current solar cells [3, 4]. Solar energy is inconsistent due to its dependence on weather, location, and time of day. Temperature difference, or thermal gradient, can generate electrical energy via the thermoelectric effect. A commercial thermoelectric energy harvester has achieved 0.29 W cm^{-2} PD from a 200 °C temperature difference [5]. But its output power degrades proportionally with respect to the temperature difference. Electromagnetic waves, especially radio frequency (RF) radiation, have been investigated as possible power sources for wireless sensor networks. A typical RF energy harvester consists of an antenna, an impedance matching circuit, and a

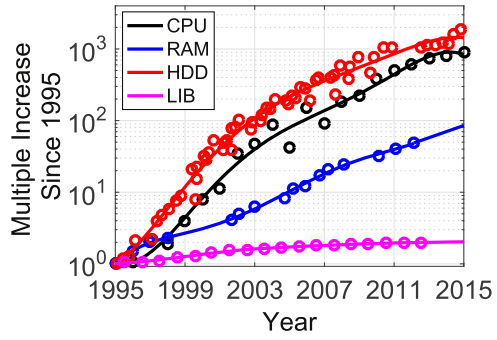

Figure 1. Relative improvements in computer technology from 1995 to 2015. The intel central processing unit (CPU) is evaluated in terms of the transistors count per integral circuit chip; the speed of random-access memory (RAM) is evaluated in terms of module bandwidth; the Seagate hard disk drive (HDD) is evaluated in terms of Gigabits per square inch; the Li-ion battery (LIB) is evaluated in terms of energy storage density (W h l^{-1}).

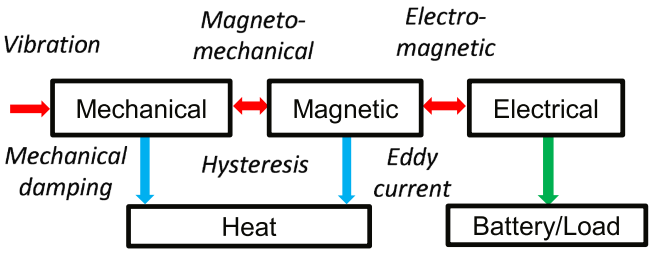

Figure 2. Energy flow within a magnetostrictive energy harvester.

voltage rectifier [6]. The output power available from RF energy harvesters is usually in the microwatt level and the performance of these devices drops off rapidly as the distance from the RF source is increased [7].

Structural vibrations can be a consistent source of waste energy, though the frequency and amplitude of structural vibrations can vary significantly. Vibrations in buildings or bridges have low frequencies ($\leqslant$0.1 Hz) and low amplitudes ($\leqslant$0.1 g); most vibrations found in household appliances such as microwave ovens and kitchen blenders have moderate frequencies (up to 150 Hz) and amplitudes ($\leqslant$0.5 g) [8]. In automobiles and rotorcraft, the vibration amplitude is relatively high while the frequency depends heavily on operating conditions [9]. For instance the vibration frequency of a light truck's engine ranges from 30 to 700 Hz depending on engine speed [10].

Due to the range of structural vibration sources, multiple types of harvesters have been developed in the literature. Vibration energy harvesters using passive materials can be classified as electromagnetic or electrostatic. The electromagnetic harvesters consist of coils and permanent magnets. Vibration sources induce relative motion between the coil and the permanent magnet, thus generating AC voltage across the coil due to Faraday's law [11, 12]. The electrostatic energy harvesters are essentially variable capacitors formed by a pair of movable electrodes with a dielectric layer in between. The electrodes are initially charged. As a result of source vibrations, the distance between the electrodes changes dynamically, which induces AC currents [13–16].

Compared with passive energy harvesters, active materials coupling mechanical energy with other energy forms can help reduce system mass and bulk. Existing active vibration energy harvesters are mainly based on piezoelectric and magnetostrictive materials [17, 18]. Piezoelectric energy harvesters are capacitive power sources with high output impedance, thus power management circuits are necessary in order to drive electrical loads. Magnetostrictive energy harvesters, which are inductive, can provide low impedance at the fundamental frequencies of common structural vibration sources. Various types of energy harvesters are compared in table 1.

This article reviews the state of the art of vibration energy harvesters based on magnetostrictive materials, especially Galfenol and Terfenol-D. Comparing the effectiveness of these devices is difficult due to the lack of universal performance metrics, and thus multiple performance metrics reflecting the properties of mechanical excitations and different configurations are proposed in this study. Advanced techniques that can reduce system mass and expand frequency bandwidth are discussed. Recent developments on magnetostrictive energy harvester modeling, including material-level models, lumped parameter models, and finite element (FE) models, are summarized to guide future device development.

2. Energy harvesting mechanism

As shown in figure 2, magnetostrictive harvesters extract electrical energy from vibration sources in two steps: (1) mechanical energy is transferred to magnetic energy via the magneto–mechanical coupling of magnetostrictive materials; (2) magnetic energy is converted to electrical energy via the electro-magnetic coupling on electrical circuits.

The magneto–mechanical coupling can be described by the Stoner–Wohlfarth approximation, where the magnetostrictive material is assumed to be a collection of non-interacting magnetic domains, as shown in figure 3 [20]. Each magnetic domain exhibits a uniform local magnetization M_s. The bulk magnetization is a weighted sum of local responses, which are determined by stress- and field-dependent domain orientations. When the mechanical compression dominates, as shown in figure 3(a), magnetic domains are forced to align in a direction perpendicular to the stress direction and thus induce zero bulk magnetization. When the magnetic field dominates, as shown in figure 3(c), magnetic domains are aligned parallel to the field direction and thus create a maximum bulk magnetization M_s. Magnetostrictive materials exhibit the maximum magneto–mechanical coupling effect, which corresponds to a 90° domain rotation, when the mechanical energy and magnetic energy are balanced. The mechanical stress in magnetostrictive vibration energy harvesters is determined by the vibration sources. Hence, a bias magnetic field H_0, as shown in figure 3, is applied to balance the mechanical energy. In magnetostrictive vibration energy harvesters, the bias magnetic field is usually generated by

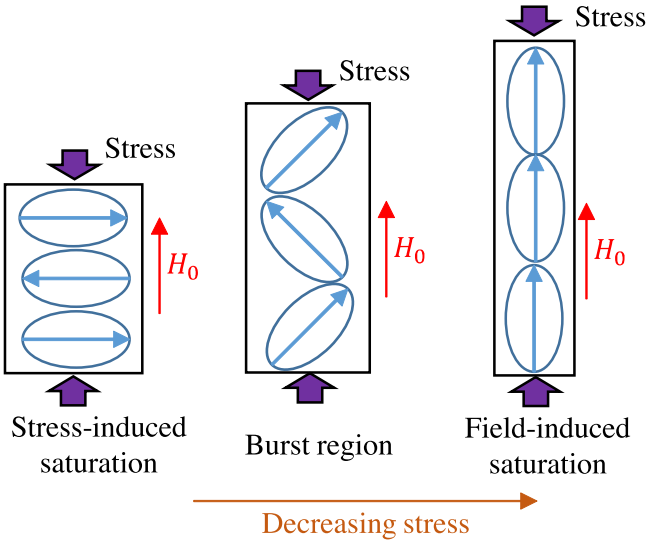

Figure 3. Magnetic domain rotation in magnetostrictive materials.

permanent magnets; the mechanical stress is either applied directly by the vibration source or indirectly by vibration-induced inertia forces. For small coaxial stress and magnetic field perturbations, the nonlinear magneto–mechanical coupling can be described by

$$\Delta B = d\Delta T + \mu^H \Delta H, \quad \Delta S = s^H \Delta T + d\Delta H, \tag{1}$$

where d is the piezomagnetic constant, s^H is the elastic compliance, μ^H is the magnetic permeability, ΔH is the magnetic field increment, ΔT is the stress increment, ΔB and ΔS are the corresponding increments of flux density and strain along the input direction, respectively.

The electro–magnetic coupling is established by pickup coils placed around the magnetostrictive element. The bulk magnetization variation and corresponding flux density variation can generate usable electrical voltage on the coils via Faraday's law,

$$V = -N_c A_c \frac{\partial B}{\partial t} = -\mathrm{d}N_c A_c \frac{\partial T}{\partial t}, \tag{2}$$

where A_c is the coil's cross section and N_c is the total number of turns. In contrast to capacitive piezoelectric harvesters, magnetostrictive energy harvesters are inductive. As such, they can provide low output impedance at the fundamental frequencies of common structural vibration sources, and thus can directly drive electrical loads or charge a battery. AC–DC converters and battery charging circuits have been developed for magnetostrictive harvesters [19]. To simplify the analysis, a resistive load R_L is attached to the pickup coil and energy storage units are ignored. The joule heat dissipated on R_L is assumed to be the energy harvested.

3. Performance metrics

According to the stress state in the magnetostrictive element, magnetostrictive energy harvesters can be classified as an axial type and a bending type. Besides the system configuration, the performance of magnetostrictive energy harvesters depends on multiple factors including the vibration source and the volume of active material. Performance metrics considering some or all of these factors are summarized in this section.

3.1. Energy conversion efficiency η

The energy conversion efficiency η is defined as

$$\eta = \frac{W_{\text{out}}}{W_{\text{in}}}, \tag{3}$$

where W_{out} is the electrical energy consumed or stored by the electrical circuit and W_{in} is the total mechanical energy input. The energy conversion efficiency η is calculated based on different excitation types. For impulsive excitations,

$$W_{\text{out}} = \int_0^{+\infty} \frac{V_L(t)^2}{R_L} \mathrm{d}t, \tag{4}$$

where $V_L(t)$ is the voltage across R_L. The total mechanical energy input is

$$W_{\text{in}} = 0.5 F_0 D_0, \tag{5}$$

where F_0 is the amplitude of the impulsive force and D_0 is the initial deflection due to the applied force [21]. For periodic force excitations,

$$W_{\text{out}} = \int_0^{T_0} \frac{V_L(t)^2}{R_L} \mathrm{d}t, \tag{6}$$

where T_0 is the period of the input stress. The total mechanical energy input per cycle is

$$W_{\text{in}} = \int_0^{T_0} F(t)\dot{D}(t)\mathrm{d}t, \tag{7}$$

where $D(t)$ is the corresponding displacement induced by the input force $F(t)$. The energy conversion efficiency is equivalent to the loss factor induced by magneto–mechanical coupling, which is important for magnetostrictive damper development. Detailed discussions on the loss factor have been presented in [22]. Since the mechanical energy available from structural vibrations (e.g. base acceleration input) is typically unlimited, the energy conversion efficiency is only suitable for force excitations.

3.2. Power density (PD)

The output power generated by a unit volume of magnetostrictive material, also known as PD, has been implemented in the literature [19, 21, 23, 24].

$$\text{PD} = \bar{P}/V_a, \tag{8}$$

where V_a is the volume of active material and $\bar{P}$ is the average output power. PD is applicable to periodic excitation, where

$$\bar{P} = \frac{W_{\text{out}}}{T_0}. \tag{9}$$

However, this metric is incomplete, because it does not take the properties of energy sources, such as excitation frequency and amplitude, into consideration.

Table 1. Comparison between vibration energy harvesters [19].

Type	Advantages	Disadvantages
Electromagnetic	■ passive materials ■ low output impedance	■ bulky pickup coils ■ bulky magnets
Electrostatic	■ passive materials ■ compatible with MEMS	■ need external voltage/charge sources ■ high output impedance ■ charge leakage
Piezoelectric	■ compatible with MEMS ■ high coupling coefficient	■ depolarization/aging ■ brittle bulk piezolayer ■ flexible PVDF with low coupling ■ high output impedance ■ charge leakage
Magnetostrictive	■ high coupling coefficient ■ no depolarization/aging ■ high mechanical strength (Galfenol/Metglas/Alfenol) ■ low output impedance ■ high frequency application ■ can possibly be compact (through microscale deposition)	■ highly nonlinear ■ bulky bias magnets and pickup coils

3.3. Normalized PD_{norm} [25]

The kinetic energy of a sinusoidal vibration source is proportional to A_0^2/f_0^2, where A_0 is the base acceleration amplitude and f_0 is the excitation frequency. To exclude the source dependence, the average output power can be normalized as

$$\mathrm{PD_{norm}} = \mathrm{PD}\frac{f_0^2}{A_0^2}. \tag{10}$$

The normalized PD only considers the volume of active materials but not the size or mass of the device, which are essential in practice, especially in aircraft applications.

3.4. Axial effectiveness (AE) [26]

An AE considering device mass, electrical load dependence, and mechanical damping has been developed for the axial type energy harvester, where the stress is uniformly distributed inside the magnetostrictive element. Assuming the magnetostrictive element operates in the linear region (small signal assumption) and its hysteresis is negligible, the AE is [26]

$$\mathrm{AE} = k^2Q^2\left(\frac{\rho}{\rho_0}\right)\frac{\eta}{\eta_{\max}}, \tag{11}$$

where k is the coupling coefficient of the transducer, Q is the quality factor, ρ_0 is the reference material density, ρ is the actual density of the device, η is the energy conversion efficiency, and $\eta_{\max}$ is the maximum theoretical energy conversion efficiency available from the system. This metric ignores the system damping induced by the magneto–mechanical coupling and only applies to a narrow frequency range around system resonance.

3.5. Generalized effectiveness (GE) [18]

A GE has been proposed for both axial and bending type energy harvesters as [18]

$$\mathrm{GE} = \frac{\bar{P}}{0.5Y_0Z_l\omega^3m}, \tag{12}$$

where Y_0 is the displacement amplitude of base excitation, Z_l is the maximum tip deflection for harvesters in bending type or the axial deformation for harvesters in axial type, and ω is the base excitation frequency in rad s^{-1}. Depending on the design constraints, m denotes the total volume or total mass of the harvester. The value of GE describes the performance of energy harvesters subjected to fixed sinusoidal base excitations or force inputs, but the frequency bandwidth is excluded.

3.6. Normalized effectiveness GE_{norm}

Taking the device's frequency bandwidth BW into account, Mitcheson *et al* [18] normalized the GE as

$$\mathrm{GE_{norm}} = \mathrm{GE}\frac{\mathrm{BW}}{\omega}. \tag{13}$$

Table 2 provides guidelines for the performance metric selection in future magnetostrictive energy harvester studies.

4. Magnetostrictive energy harvester configurations

4.1. Axial type

A typical axial type magnetostrictive energy harvester is presented in figure 4. Berbyuk [27] inserted a 6.35 mm diameter and 50 mm long Galfenol (at 18.4% Ga) rod into a

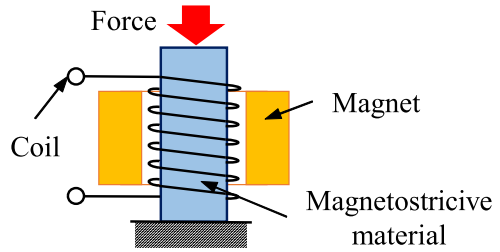

Figure 4. Configuration of axial type magnetostrictive energy harvesters.

4000 turn copper coil and achieved a maximum output power of 0.45 W under a 60 Hz, 55 MPa amplitude sinusoidal stress. Deng [28] designed a harvester using a solid Terfenol-D rod with a diameter of 7 mm and a length of 10 mm, as shown in figure 5(a). A 750 Hz, 7.3 MPa amplitude sinusoidal axial stress was applied on the device and a resistive load of 31 Ω was attached to the 500-turn pickup coil. The induced voltage across the load is presented in figure 5(b), which corresponds to an average output power of 73.15 mW.

One of the main applications of these devices is to scavenge electrical energy from impact excitations. Zhang [30] presented an axial type harvester, as shown in figure 6, to collect energy from human walking. Modeling results showed that the maximum output power is 0.09 W m^{-2}. The pre-stress spring in figure 6 protects the brittle Terfenol-D rod from cracking. Without the pre-stress spring, the Terfenol-D rod cracked within 150 cycles and resulted in an output voltage degradation by 5% [31]. In practice, the pre-stress is adjusted in accordance to the permanent magnet strength such that the magnetostrictive material operates in the burst region. The energy harvester presented in figure 6 has been installed and tested inside vehicle tires by Liu *et al* [32]. Yan *et al* [33, 34] later utilized a flextensional cage to provide pre-stress on the magnetostrictive component, as shown in figure 7. The maximum output voltage was 2.17 V for a 10 MPa impact excitation, when a 15 mm diameter and 40 mm long Terfenol-D rod was employed.

Axial type magnetostrictive energy harvesters are now commercially available. Figure 8 presents ocean wave generators in two configurations [35, 36]. The energy cost from these devices is reported as 2–4 cents per kWh [35]. Figure 9 presents another magnetostrictive energy harvester located in the sealed bearing portion of a downhole drill [37]. The drill motion induces a low frequency unidirectional deformation and a high frequency reciprocating deformation on the magnetostrictive component, introducing a bias stress and causing a dynamic flux density variation, respectively. A coil embedded into the electronics converts flux density variation into electrical energy.

One of the drawbacks associated with the axial type vibration energy harvester is that it requires a large axial force. To resolve this issue, Staley and Flatau [38, 39] incorporated an axial type energy harvester with a long cantilever beam, as shown in figure 10. Magnified by the leverage (cantilever beam), the inertia force on the tip mass is able to induce large axial stress on the magnetostrictive rod.

The other drawback is that the frequency bandwidth of the axial type energy harvester is limited due to mechanically-induced eddy currents [40]. Laminated magnetostrictive materials have been investigated to enhance dynamic performance. Berbyuk and Sodhani [41] implemented a 15 mm diameter and 50 mm long laminated Terfenol-D rod to construct the energy harvester shown in figure 4. A maximum energy conversion efficiency of 25% was achieved at 500 Hz.

4.2. Bending type

Most axial type magnetostrictive energy harvesters need to be installed in the load path and exhibit limited frequency bandwidth. In contrast, the bending type energy harvesters are ideal for collecting energy from any vibrating surfaces. Configurations of magnetostrictive components in existing bending type energy harvesters include a single layer magnetostrictive beam, a bimorph beam (two layers of magnetostrictive materials), and a unimorph beam (magnetostrictive and passive material composites).

Studies on the single layer magnetostrictive beam mainly targeted tip force excitations. Figure 11 shows an energy harvester prototype that can scavenge electrical energy from a rotating shaft [42]. The beam is excited by a transverse magnetic force on its tip. A 300 rpm rotating shaft with 12 evenly-distributed permanent magnets is able to generate a peak voltage of 0.5 V [42]. Zucca *et al* [43] presented an similar structure, as shown in figure 12, where the magnetostrictive beam was excited by a longitudinal tip force. A maximum power of 18 μW was achieved under a 300 Hz, 1 MPa amplitude sinusoidal axial stress [43]. In the single layer magnetostrictive beam designs, the bending deformation induces compression in half of the beam while causing tension in the other half. The stress-induced flux density variation in each half cancels out and thus the output power available from this configuration is minimal.

Ueno and Yamada [21] proposed a Galfenol bimorph harvester, which consists of two parallel Galfenol beams, as shown in figures 13(a) and (b). The gap between the two Galfenol layers provides enough space for a pair of pickup coils. By ignoring the shear deformation, each Galfenol layer operates purely in tension or, alternatively, purely in compression. Similar to the axial type harvesters, tensile or compressive stress in the magnetostrictive layer is able to cause flux density variation, which then induces electrical voltage in the pickup coils. Experimental results have shown that the energy conversion efficiency of this device can reach 16% [21]. However, the output power of the bimorph configuration is relatively small due to two reasons: (1) the shear deformation that reduces the flux density variation is significant and (2) the magnetostrictive beam is saturated by the tensile stress and thus cannot generate any electrical energy in half a cycle, as shown in figure 13(c).

Kita *et al* [44] has recently developed a unimorph energy harvester, as shown in figure 14, where the coil was only wound around the Galfenol layer. The maximum energy conversion efficiency is 35% under a 202 Hz, 25 N impulsive tip force [44]. The same unimorph configuration can be improved by rearranging the bias magnets and reshaping the passive layer. Figure 15

Table 2. Summary of existing performance metrics used for magnetostrictive harvesters.

Metrics	Excitation	Advantages (■) and limitations (□)
η	Impulsive force Periodic acceleration	■ dimensionless ■ ranging from 0 to 1 □ not consider device's mass/size or external circuit
PD	Periodic force/acceleration	■ consider the size of the active material □ not eliminate source influence □ not consider system size/mass □ not include external circuit
PD_{norm}	Sinusoidal acceleration	■ consider the size of the active material ■ eliminate source influence □ not include external circuit
AE	Sinusoidal force/acceleration	■ dimensionless ■ eliminate source dependence ■ include device's mass and harvesting circuit □ one-way coupled magnetomechanical effect □ small signal assumption □ only works at resonance
GE	Sinusoidal acceleration	■ dimensionless ■ range from 0 to 1 ■ include packaging size and device's mass □ one-way coupled magnetomechanical effect
GE_{norm}	Sinusoidal acceleration	■ dimensionless ■ include frequency bandwidth □ sine sweep test needed

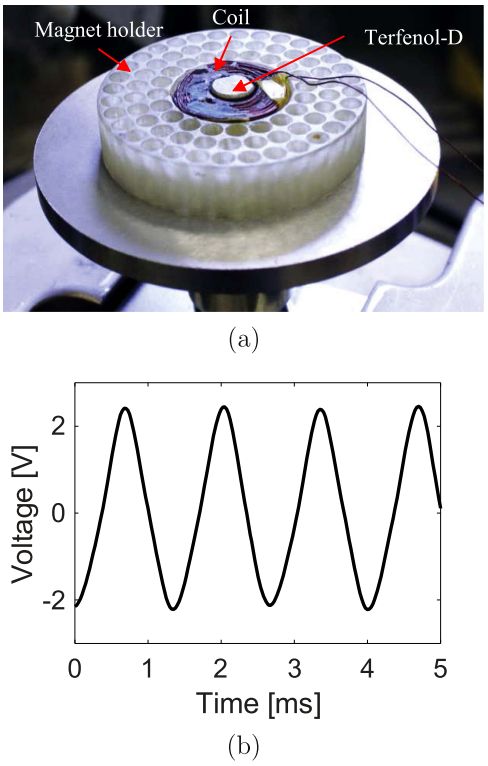

Figure 5. Axial type vibration energy harvester based on Terfenol-D: (a) physical assembly and (b) voltage across the resistive load ($R_L = 31\ \Omega$) when a 750 Hz, 7.3 MPa amplitude sinusoidal axial stress is applied [29].

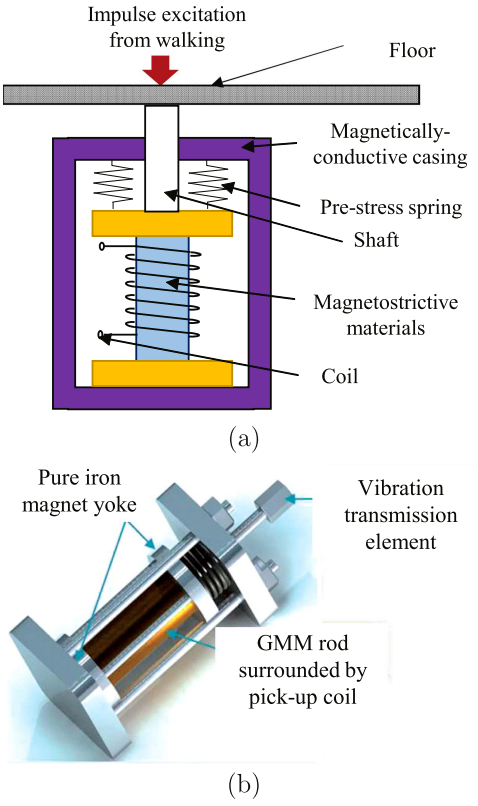

Figure 6. Configuration of axial type magnetostrictive energy harvesters with pre-stress springs: (a) cross-section view and (b) 3D assembly [30–32].

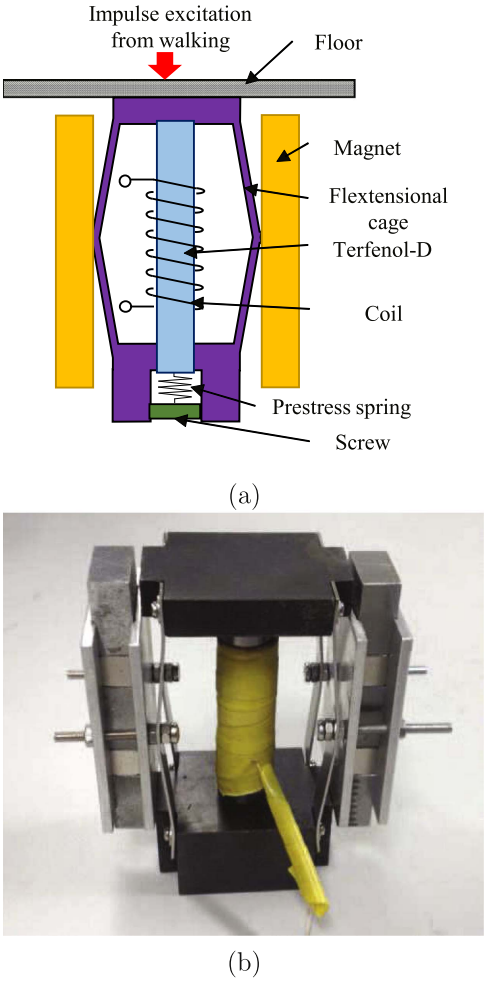

Figure 7. Configuration of axial type magnetostrictive energy harvesters with a flextensional cage: (a) cross-section view and (b) physical assembly [33, 34].

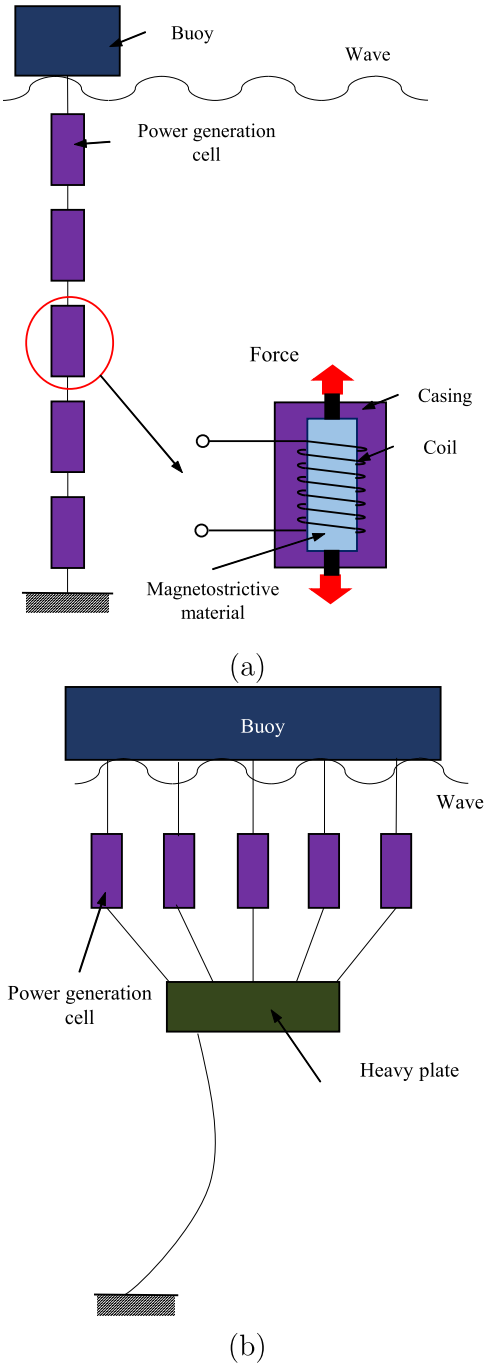

Figure 8. Configurations of ocean wave energy harvesters: (a) fixed base [35] and (b) movable base [36].

presents a U-shape energy harvester developed by Ueno [45] where the permanent magnets were mounted on the base. As the top beam vibrates, the gap between the magnet and the top beam changes thus introducing additional flux density variation across the pickup coil. The average output power reaches 3.7 mW under a 166 Hz, 24.5 m s^{-2} amplitude sinusoidal base excitation. This device has also been implemented to harvest energy from finger tapping, as shown in figure 16, where a maximum energy of 0.7 mJ has been scavenged from a single tap.

Similar to the bimorph energy harvesters, the thin Galfenol layer in the aforementioned unimorph suffers severe shear deformation. Wang and Yuan [19] eliminated the shear stress by bonding magnetostrictive Metglas layers directly on top of passive non-magnetic beams. An electrical circuit containing an AC to DC rectifier and a DC to DC converter was also developed [19]. The average PD was 576 μW under a 1.1 kHz, 8.06 m s^{-2} amplitude sinusoidal base excitation [19]. Yoo and Flatau [23] later created a similar Galfenol unimorph harvester and evaluated its performance under various base excitations, as shown in figure 17(a). The Galfenol beam was mounted beneath the brass beam such that the initial bending induced by the tip mass could create a pre-compression in the Galfenol layer. Hence, the unimorph harvester can generate electrical energy in a full cycle, as shown in figure 17(b). In addition, the tip magnet vibrates relative to the pickup coil and could generate extra electrical voltage on top of the voltage induced by the magneto-mechanical coupling. However, the bending type harvesters in most previous studies were tested too close to the electromagnetic shaker [19, 23, 44], and the influence of magnetic flux leaked from the shaker's solenoid was not completely eliminated. Deng and Dapino [24, 25, 46] developed an improved experiment by shielding the unimorph from the shaker, as shown in figure 17(c), and enhanced output PD

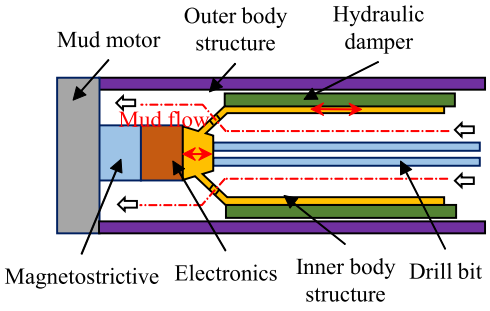

Figure 9. Configuration of a magnetostrictive energy harvester on a downhole drill [37].

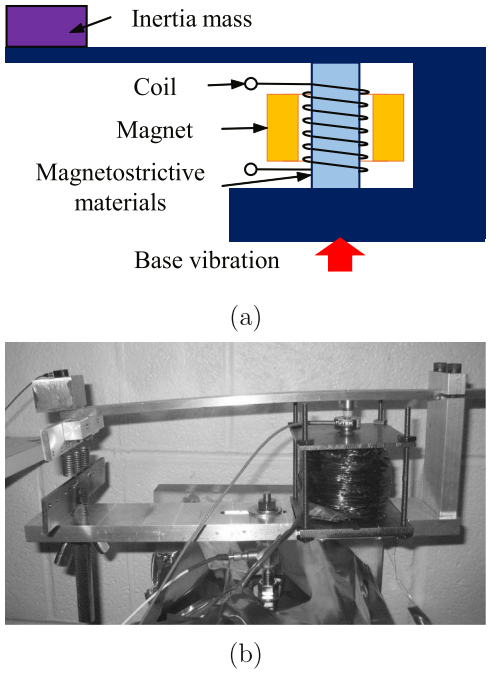

Figure 10. Incorporation of axial type magnetostrictive energy harvesters with a cantilever beam: (a) schematic and (b) physical assembly [39].

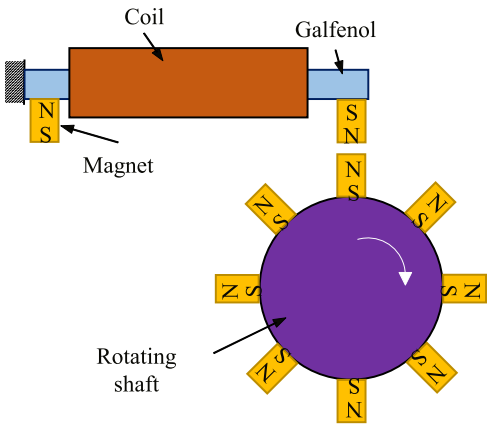

Figure 11. Configuration of a rotation energy harvester [42].

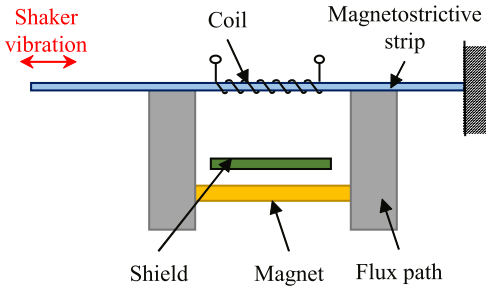

Figure 12. Configuration of an axial type energy harvester targeting longitudinal input force [43].

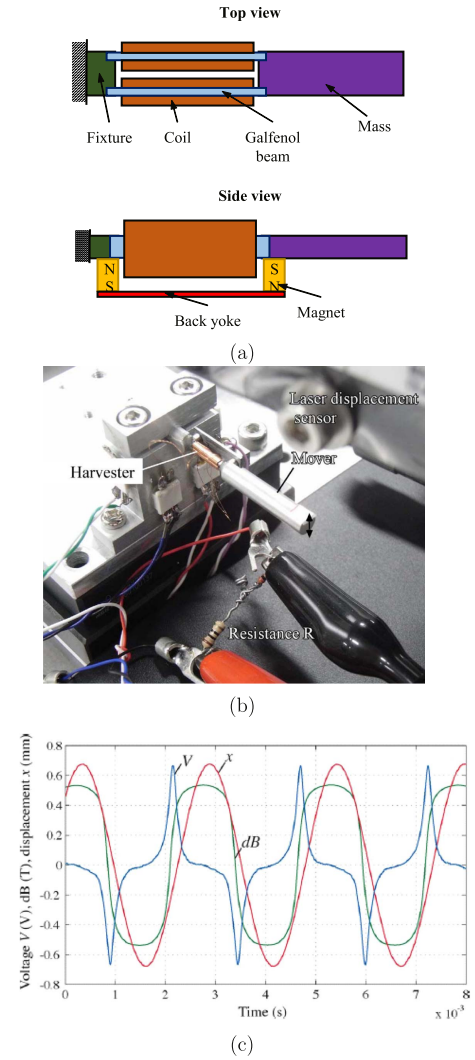

Figure 13. Configuration of a bimorph magnetostrictive energy harvester: (a) schematics, (b) physical assembly, and (c) experimental results, where V denotes the voltage across a 30 Ω resistive load, x is the tip displacement, and dB is the flux density variation measured from the coils [21].

through electrical impedance matching. A maximum output power of 0.45 W was achieved under a 139.5 Hz, 3 m s^{-2} sinusoidal base excitation [25].

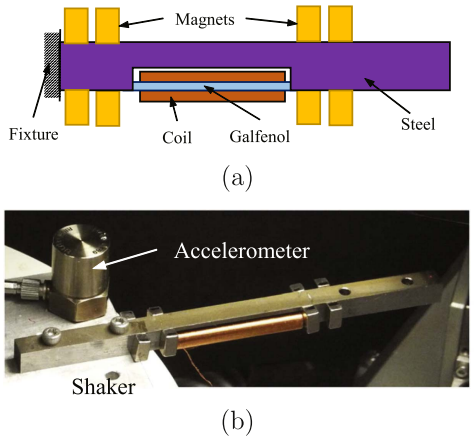

Figure 14. Configuration of a bimorph magnetostrictive energy harvester: (a) schematics and (b) physical assembly [44].

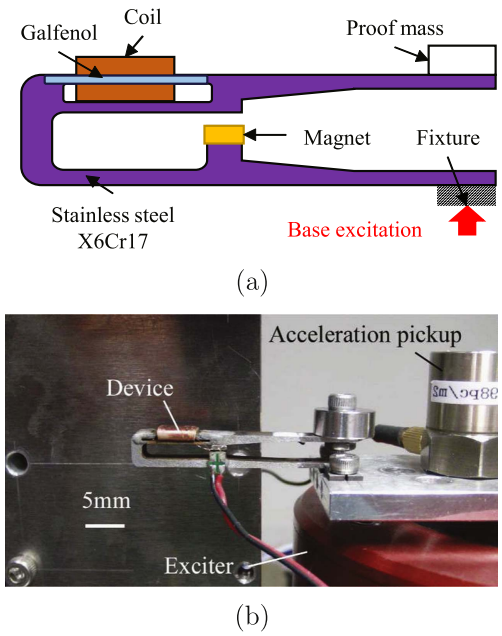

Figure 15. Configuration of a U-shaped magnetostrictive unimorph harvester under base excitation [49]: (a) schematics and (b) physical assembly.

4.3. Comparison of magnetostrictive harvesters

The performance (experimental results only) of existing magnetostrictive vibration energy harvesters under force excitation and base displacement excitation is compared in tables 3 and 4, respectively. Due to the lack of information in the literature, AE, GE, and normalized effectiveness GE_{norm} are not presented.

5. Advanced techniques in magnetostrictive energy harvesters

5.1. Hybrid energy harvester

Current magnetostrictive energy harvesters require pickup coils to convert magnetic flux variation to electrical energy.

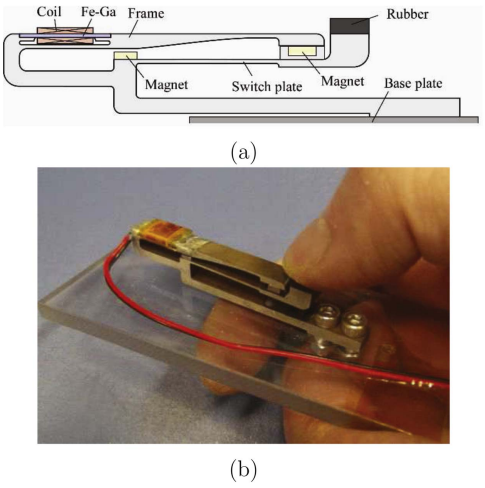

Figure 16. Configuration of a U-shaped magnetostrictive unimorph harvester for finger tapping: (a) schematics and (b) physical assembly [49].

Thus, the existing concepts of magnetostrictive harvesters cannot be implemented in micro electro-mechanical systems. A magnetoelectric composite, which consists of a piezoelectric layer sandwiched between two Terfenol-D layers, has been developed to eliminate the bulky and heavy pickup coil. Li *et al* [50, 51] proposed a magnetoelectric beam, as shown in figure 18. The composite oscillates in the magnetic field generated by a pair of permanent magnets. As the magnetic field through the beam varies, Terfenol-D layers deform and thus stress the piezoelectric layer, where electric charges are generated. Issues associated with piezoelectric energy harvesters (e.g. high output impedance and aging) still exist in this concept. As an energy harvester, magnetoelectric composites exhibit relatively low energy conversion efficiency and PD. Hence, this concept is commonly implemented in sensing [52] or wireless charging [53].

Magnetostrictive energy harvesters have also been incorporated with electromagnetic harvesters to improve the output power, as shown in figure 19. The inertia force due to the moving casing stresses the Galfenol disk and thus produces electrical voltage in the secondary coils. Simultaneously, a cylindrical magnet oscillates in the center along a steel shaft and thus creates electrical voltage in the primary coil.

5.2. Broadband harvester

Practical sources of vibration energy are typically wideband [8]. Hence, one of the key challenges for vibration energy harvesters is to scavenge energy effectively over a broad frequency range.

Mori *et al* [55] designed a bending type energy harvester based on Terfenol-D, as shown in figure 20. The position of the movable proof mass can be manually adjusted and thus the resonance of the harvester can be tuned to the base excitation frequency. Ueno [49] developed a L-shaped Galfenol unimorph harvester, as shown in figure 21, whose horizontal mode and the vertical mode are at 307 and 346 Hz,

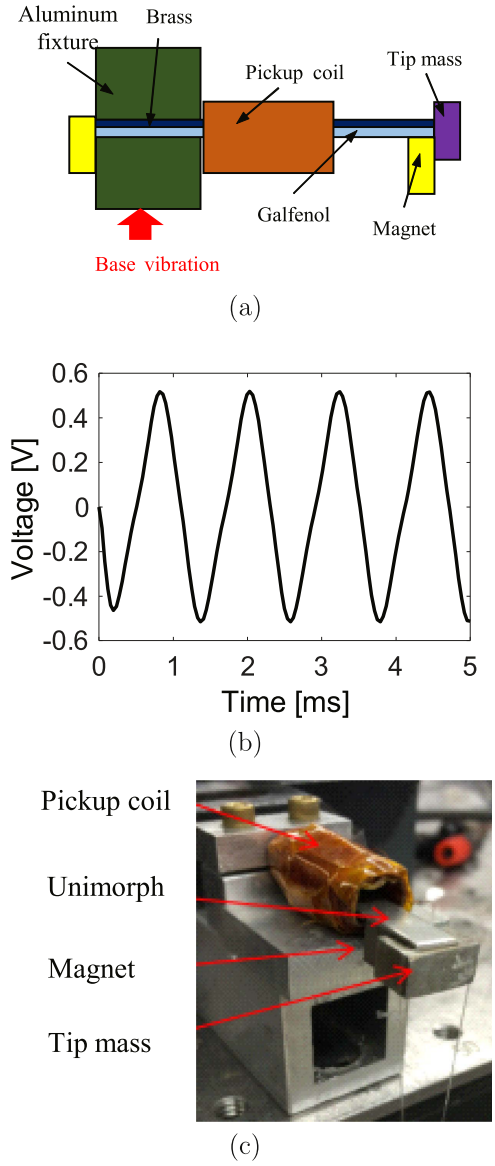

Figure 17. Configuration of unimorph magnetostrictive energy harvesters: (a) schematics, (b) open-circuit voltage across the pickup coil, and (c) physical assembly [25].

respectively. Hence, the energy harvester can effectively scavenge energy between two modes. Tsutsumi *et al* [56] created a similar L-shaped Metglas-based unimorph beam where the natural frequency ratio of the vertical and horizontal modes was tuned to be 1:2. The frequency bandwidth is expanded due to the interplay between two modes.

Nonlinear bistable structures have been developed for piezoelectric energy harvesters to improve frequency bandwidth [16, 57]. Bistable systems can transform from one stable state to the other and thus inducing large motion. The bistable nonlinear vibration of a cantilever beam can be described by [25]

$$m\ddot{x} + c\dot{x} + kx = mA_0\cos(\omega t) + F_y(x), \tag{14}$$

where m, c, and k are the equivalent mass, damping ratio, and stiffness, respectively. The amplitude and frequency of the base excitation are A_0 and ω, respectively. The nonlinear tip force $F_y(x)$, which is usually applied by repelling permanent magnet pairs [58, 59] or buckled beams [60], can be approximated by an odd polynominal function of the tip displacement x

$$F_y(x) = a_1x + a_3x^3 + h(x^5). \tag{15}$$

Ignoring the higher order terms, (14) can be written as the Duffing equation by rescaling t and x [25]

$$\ddot{X} + \gamma\dot{X} - \frac{1}{2}(1 - X^2)X = f\cos(\Omega\tau), \tag{16}$$

where

$$X = x/a_0, \quad \tau = t/\omega_0, \quad \gamma = C\omega_0/M, \quad f = A_0\omega_0^2/a_0, \quad \Omega = \omega\omega_0, \quad a_0 = \left(\frac{K - a_1}{a_3}\right)^{1/2}, \quad \omega_0 = \left(\frac{0.5M}{a_1 - K}\right)^{1/2}. \tag{17}$$

Depending on the level of excitation energy, the bistable structure described in (16) oscillates either periodically or chaotically. When the excitation energy is small and cannot drive the system away from an equilibrium position, the structure oscillates in a low-energy orbit around one of the equilibrium positions thus creating small amplitude motion, as shown in figure 22(a). When the excitation energy is large enough such that the system can jump freely between two equilibrium positions, the structure reaches a high-energy orbit surrounding both equilibrium positions, as shown in figure 22(c). For moderate excitation energy, the bistable system switches between two equilibrium positions chaotically, as shown in figure 22(b). The high-energy orbit and chaotic responses are able to create large amplitude motion and thus have been investigated to improve system bandwidth. Due to the limited magnitude of magnetic force, the repelling permanent magnet configuration has only been applied to soft cantilever beams with natural frequencies of about 10 Hz [58, 59]. The large buckled force is able to create a bistable system with a natural frequency of several hundreds of Hertz. Deng and Dapino [25] recently developed a bistable Galfenol unimorph harvester, as shown in figure 23, where the beam is initially buckled due to the longitudinal clamping force. The hardening effect on the buckled beam reduces the normalized peak PD at resonance but extends the frequency range from 1.5 to 10.5 Hz, as shown in figure 24.

6. Modeling of magnetostrictive energy harvesters

6.1. Magnetostrictive material model

Magnetostrictive materials exhibit significant nonlinearities including anisotropy, saturation, and hysteresis, and thus (1) is inaccurate to describe the magneto–mechanical coupling. Fully-coupled nonlinear constitutive models have been developed in previous studies.

Table 3. Comparison of existing magnetostrictive energy harvesters under force excitations. For impulsive input, the frequency value presented is the resonant frequency of the device; for periodic input, the frequency value denotes the fundamental frequency of the force wave.

Author	Active material	Harvester and excitation types	Freq. (Hz)	Force amp. (N)	Volume (cm^3)	$\bar{P}_{out}$ (mW)	η (%)	PD (mW cm^{-3})
Adly [47]	Terfenol-D rod	Axial, sinusoidal	50	310	1.62	0.43	NA	0.27
Berbyuk [41]	Terfenol-D rod	Axial, sinusoidal	500	99.84	8.84	1.56×10^5	25	1.77×10^4
Berbyuk [41]	Terfenol-D rod	Axial, sinusoidal	1000	109.1	8.84	2.42×10^5	18	2.74×10^4
Berbyuk [27]	$Fe_{81.6}Ga_{18.4}$ rod	Axial, sinusoidal	60	34.84	1.58	4.5×10^2	6	2.84×10^2
Deng [25]	$Fe_{81.6}Ga_{18.4}$ unimorph	Bending, impulsive	139.5	2	0.0645	NA	5.93	NA
Deng [22]	Terfenol-D rod	Axial, sinusoidal	750	280	0.3848	73.15	19.32	190.1
Kita [44]	$Fe_{81.6}Ga_{18.4}$ bimorph	Bending, impulsive	202	24.5	0.441	NA	35	NA
Kita [44]	$Fe_{81.6}Ga_{18.4}$ bimorph	Bending, impulsive	121	24.5	0.147	NA	16	NA
Kita [44]	$Fe_{81.6}Ga_{18.4}$ bimorph	Bending, impulsive	251	24.5	0.441	NA	26	NA
Kita [44]	$Fe_{81.6}Ga_{18.4}$ bimorph	Bending, impulsive	138	24.5	0.441	NA	24	NA
Liu [32]	Terfenol-D rod	Bending, impulsive	NA	NA	3.0159	2.25 (peak)	NA	0.746 (peak)
Ueno [21]	$Fe_{81.6}Ga_{18.4}$ bimorph	Bending, impulsive	395	NA	0.01	NA	16	NA
Ueno [21]	$Fe_{81.6}Ga_{18.4}$ bimorph	Bending, impulsive	94	NA	0.01	NA	5.4	NA
Viola [31]	Terfenol-D rod	Axial, impulsive	NA	980 (0.1 s duration)	1.0053	121 (peak)	NA	121 (peak)
Zucca [43]	$Fe_{78}B_{13}Si_9$ strip	Axial, sinusoidal	300	NA	0.06	0.018	NA	0.3

Mathematical models such as the Preisach model [61] and the Prandtl–Ishlinskii model [62] built on phenomenological operators require large amounts of empirical parameters. Jiles and Atherton [63] assumed that the magnetization variation in magnteostrictive materials is induced by magnetic domain rotation, which consists of an anhysteretic component due to reversible domain wall bowing and a hysteretic component due to irreversible domain wall motion. The anhysteretic magnetization is described by an empirical Lagenvin function; the hysteretic magnetization is calculated incrementally based on an averaged pinning site density.

Armstrong eliminated the empirical operators in the aforementioned constitutive models and first derived a computationally efficient model based on thermodynamic energy principles where the Gibbs free energy G^k along kth orientation consists of three terms: anisotropic energy, magnetic energy, and magnetomechanical coupling energy. The bulk magnetization $\mathbf{M}$ and magnetostriction $\mathbf{S}$ are weighted sums of local behaviors

$$\mathbf{M} = M_s \sum_{k=1}^{r} \xi^k \mathbf{m}^k, \quad \mathbf{S} = \sum_{k=1}^{r} \xi^k \mathbf{S}_m^k, \tag{18}$$

where ξ^k is the weight or volume fraction of the kth magnetic moment orientation $\mathbf{m}^k$, r is the total number of possible moment orientations, and $\mathbf{S}_m^k$ is the local magnetostriction. The volume fraction is calculated using an energy-based Boltzmann distribution

$$\xi^k = \frac{e^{-G^k/\Omega}}{\sum_{k=1}^{r} e^{-G^k/\Omega}}, \tag{19}$$

where Ω is the Armstrong smoothing factor. Restorff *et al* [64] assumed 2048 possible moment orientations ($r = 2048$) which are equally distributed in 3D space. Atulasimha *et al* [65] assumed 98 important crystallographic orientations for $\langle 110 \rangle$-oriented Galfenol samples. Armstrong [66] utilized only 8 possible orientations for Terfenol-D. By locally defining anisotropy energy along 6 easy directions, Evans and Dapino [68] further improved the efficiency and accuracy of Armstrong's model for cubic symmetric Galfenol. Modeling results of magnetic flux density versus stress curves, whose slopes represent the magneto–mechanical coupling strength in Galfenol, are plotted on top of experimental data in figure 25.

6.2. Lumped parameter model

Figure 26 presents a typical equivalent circuit for magnetostrictive energy harvesters. The magneto-mechanical coupling effect is represented by a gyrator with a coefficient of $\mathbf{G}$. The

Table 4. Comparison of existing magnetostrictive energy harvesters subjected to base excitations (sinusoidal acceleration).

Author	Active material	Harvester types	Freq. (Hz)	Amp. ($m\ s^{-2}$)	Volume (cm^3)	$\bar{P}_{out}$ (mW)	PD ($mW\ cm^{-3}$)	PD_{norm} ($\mu Ws^2\ m^{-5}$)
Deng [25]	$Fe_{81.6}Ga_{18.4}$ unimorph	Bending	139.5	3	0.0654	0.45	6.88	14.88
Deng [24]	$Fe_{81.6}Ga_{18.4}$ unimorph	Bending	200	9.8	0.0369	0.9	24.39	10.16
Hu [48]	Metglas 2605SC	Bending	324	15	0.046	0.97	21.09	9.84
Staley [38, 39]	Terfenol-D rod	Axial	61	7	1.61	43.5	27.02	2.05
Staley [38, 39]	production grade $Fe_{81.6}Ga_{18.4}$ rod	Axial	61	6.2	1.6	16	10	0.97
Staley [38, 39]	research grade $Fe_{81.6}Ga_{18.4}$	Axial	61	6.2	1.6	30	18.75	1.82
Ueno [45]	$Fe_{81.6}Ga_{18.4}$ unimorph	Bending	212	11.8	0.007	1.2	171.43	55.33
Ueno [49]	$Fe_{81.6}Ga_{18.4}$ unimorph	Bending	166	24.5	0.39	3.7	9.49	0.44
Wang [19]	Metglas 2605SC	Bending	58	8.06	0.22	0.2	0.91	0.05
Yoo [23]	$Fe_{81.6}Ga_{18.4}$ unimorph	Bending	222	9.8	0.52	2.2	4.23	2.17

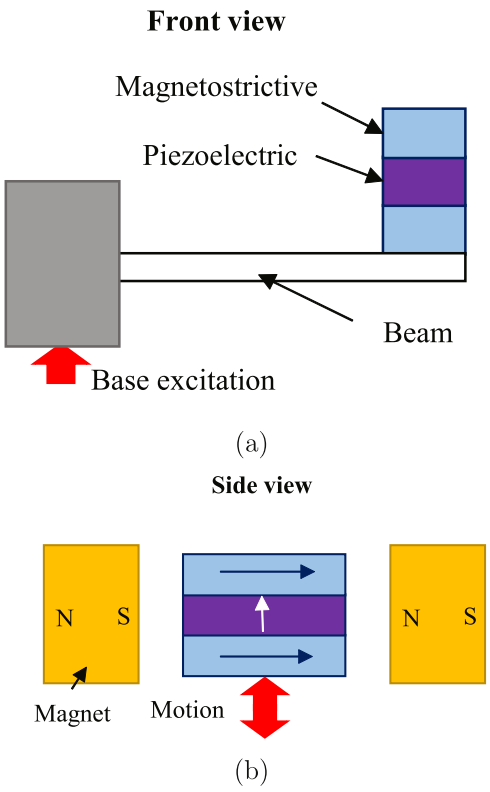

Figure 18. Hybrid vibration energy harvester based on Terfenol-D and piezoelectric materials [53].

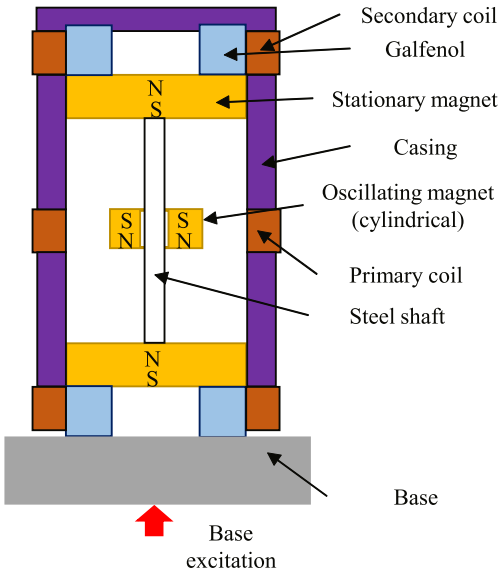

Figure 19. Hybrid vibration energy harvester combining magnetostrictive harvesters and electromagnetic harvesters [54].

system governing equations can be written as

$$\begin{aligned} \mathbf{M}_m\ddot{x} + \mathbf{C}_m\dot{x} + \mathbf{K}_m x + \mathbf{G}I &= \mathbf{F}_s, \quad \text{(Mechanical)} \\ L_c\dot{I} + R_c I + V_L &= \mathbf{G}^T\dot{x}, \quad \text{(Electrical)} \end{aligned} \tag{20}$$

where $\mathbf{M}_m$, $\mathbf{C}_m$, and $\mathbf{K}_m$ are the mass, damping, and stiffness matrices, respectively. The vector $\mathbf{F}_s$ is the mechanical input, I

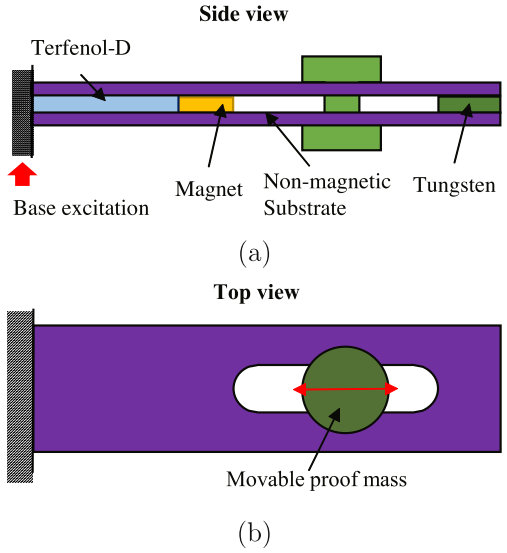

Figure 20. Tunable magnetostrictive beam harvester [55].

is the induced current in the electrical circuit, L_c is the inductance associated with the pickup coil, V_L is the voltage across the electrical load, and x is the displacement. Since the Young's modulus and permeability of magnetostrictive materials are stress- and field-dependent, the stiffness $\mathbf{K}_m$ and the coil inductance L_c are usually written as functions of the stress and magnetic field.

Lumped parameter models have been developed and validated for magnetostrictive materials bearing axial loads. Zhao and Lord [69] studied a general axial type energy harvester using the linearized material model in (1) and improve model accuracy by considering the eddy current effect and magnetic flux leakage. Since the stress distribution in the magnetostrictive layer is not uniform during bending, a single degree of freedom (DOF) equation cannot accurately capture the nonlinear behavior of the bending type devices [23]. Figure 27 presents a comparison of modeling results and measurements on the unimorph harvester developed by Yoo and Flatau [23]. Wang and Yuan [19] developed a multi-DOF lumped parameter model by dividing the bending type magnetostrictive harvester, as shown in figure 17(a), into small sections along the longitudinal direction. The magneto–mechanical coupling was linearized locally within each section and the global stiffness, mass, and damping matrices in the equivalent circuit were calculated by lumping all local sections together via the Galerkin method.

Magnetostrictive behavior can be linearized only in low signal regimes where stress and field variations are negligible. To improve the modeling accuracy under large excitations, piecewise linear lumped parameter models have been developed in which the coefficients in (1) are updated in each time interval. Clemente *et al* [70] implemented a phenomenological and anhysteresis constitutive model to calculate the stress- and field-dependent coefficients in (20). An efficient discrete energy averaged model requiring no empirical parameters has been utilized to update the coefficients of (20) in real time [71, 72]. Cao *et al* [73, 74] have recently

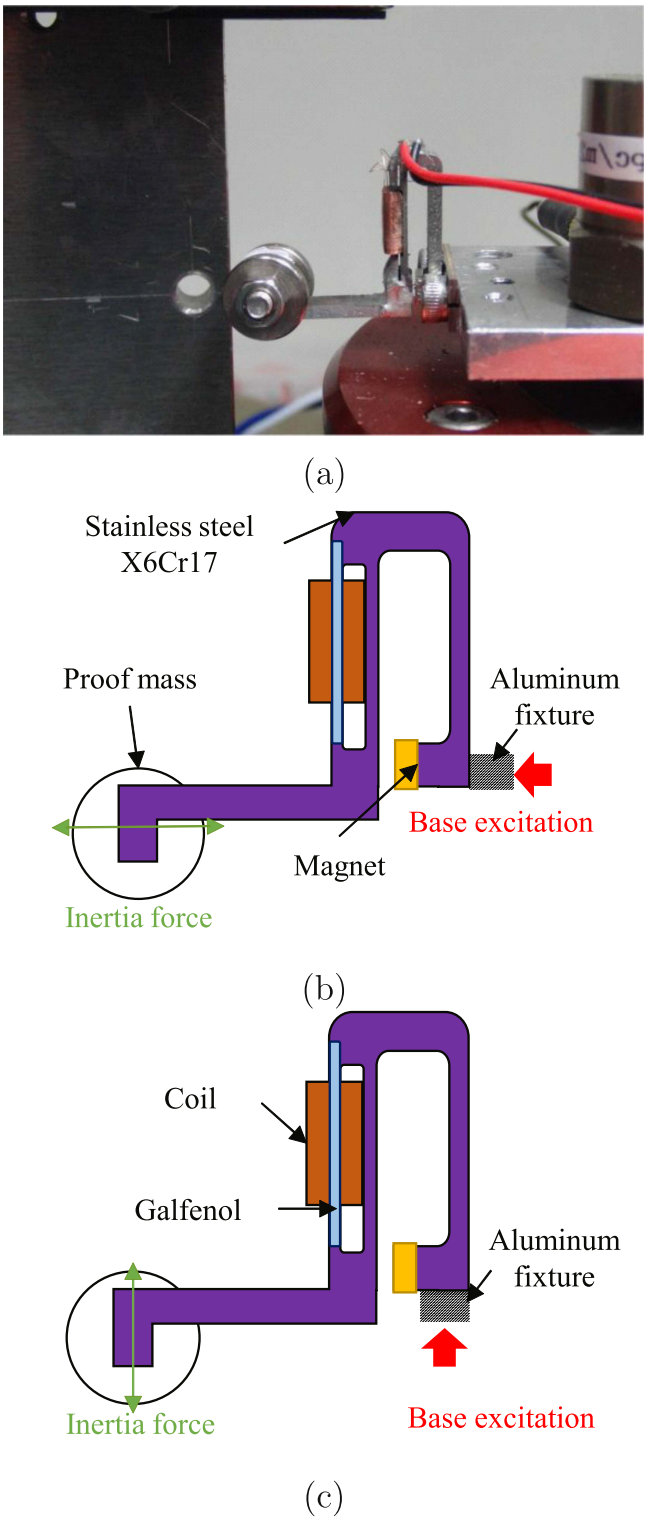

Figure 21. Schematics of L-shaped magnetostrictive energy harvesters based on Galfenol unimorphs: (a) assembly, (b) horizontal mode, and (c) vertical mode [49].

incorporated the nonlinear lumped parameter model with external energy harvesting circuits including AC/DC converters, voltage comparators, and energy storage units. Hysteresis loss in magnetostrictive materials has been added to the lumped parameter modeling framework by defining a complex stiffness coefficient [75].

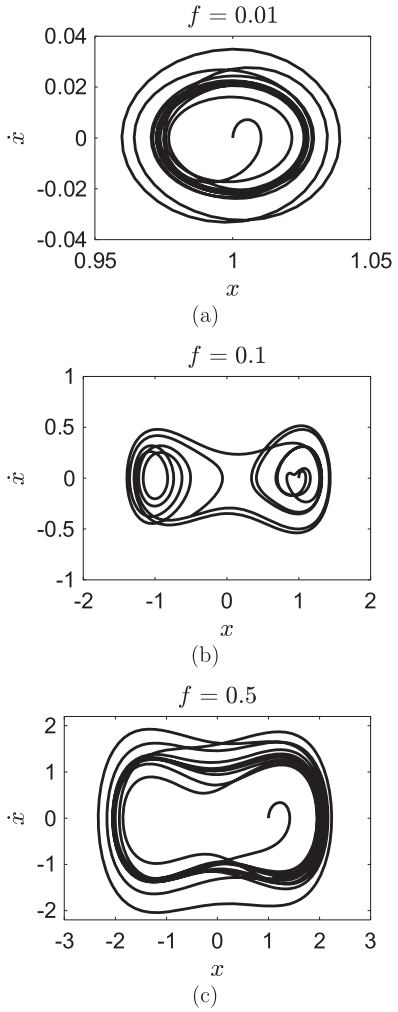

Figure 22. Phase plot of the Duffing equation (16), where $\Omega = 0.8$, $\gamma = 0.1$, and initial condition $(\dot{X}_0, X_0) = (0, 1)$: (a) $f = 0.01$, (b) $f = 0.1$, and (c) $f = 0.15$ [25].

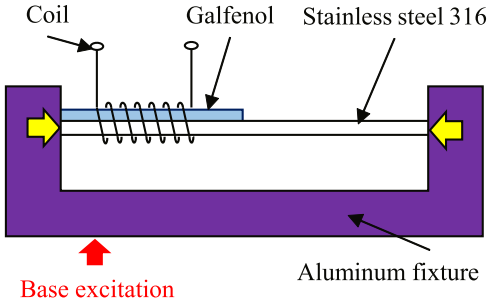

Figure 23. Configuration of a buckled Galfenol unimorph energy harvester [25].

6.3. FE model

A magnetostrictive vibration energy harvester is a highly-nonlinear system that fully couples mechanical, magnetic and electrical dynamics. In the FE framework, the mechanical dynamics is described by Newton's law

$$\int_{V_I} \mathbf{T} \cdot \nabla \delta\mathbf{u} \mathrm{d}V_I + \int_{V_I} (\rho\ddot{\mathbf{u}} + c_d\dot{\mathbf{u}}) \cdot \delta\mathbf{u} \mathrm{d}V_I = \int_{\partial V_I} (\mathbf{tn}) \cdot \delta\mathbf{u} \mathrm{d}S + \int_{V_I} \mathbf{f}_B \cdot \delta\mathbf{u} \mathrm{d}V_I, \quad (21)$$

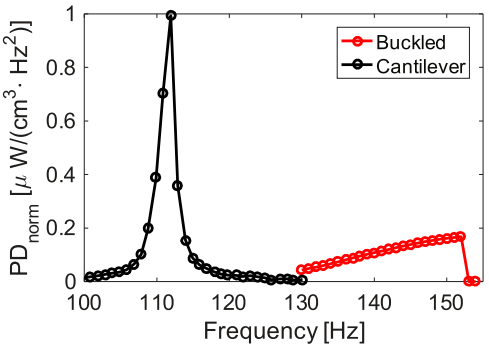

Figure 24. Normalized power density PD_{norm} with respect to the excitation frequency measured from a cantilever beam and a buckled beam [25].

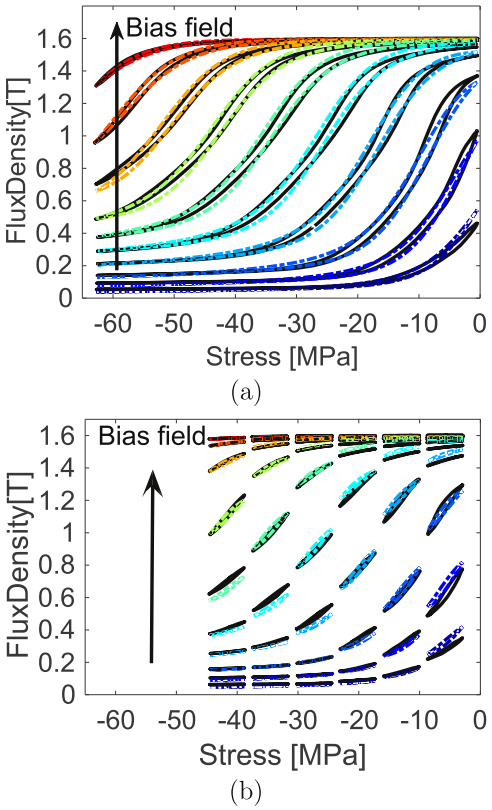

Figure 25. Comparison of the experimental (solid) and modeled (dashed) sensing responses of a ⟨100⟩-oriented, highly-textured, polycrystalline $Fe_{81.6}Ga_{18.4}$ rod to 1 Hz sinusoidal compression under constant magnetic fields of 0.73, 1.42, 2.41, 3.88, 5.50, 7.17, 8.84, 10.51, 12.19, and 13.76 kA m^{-1}: (a) magnetic flux density versus stress major loops and (b) magnetic flux density versus stress minor loops [67]. Arrows indicate increasing bias magnetic field.

where $\mathbf{u}$ is the displacement vector, T is the stress tensor, V_I denotes the integration domain, ρ is the material density, c_d is the damping coefficient, $\mathbf{t}$ is the boundary stress on the surface ∂V_I, and $\mathbf{f}_B$ is the body force. The magnetic dynamics is described by Maxwell's equation

$$\int_{V_I} \mathbf{H} \cdot (\nabla \times \delta\mathbf{A}) \mathrm{d}V_I = \int_{\partial V_I} (\mathbf{H} \times \mathbf{n}) \cdot \delta\mathbf{A} \mathrm{d}S + \int_{V_I} (\mathbf{J}_s - \sigma\frac{\partial \mathbf{A}}{\partial t}) \cdot \delta\mathbf{A} \mathrm{d}V_I, \quad (22)$$

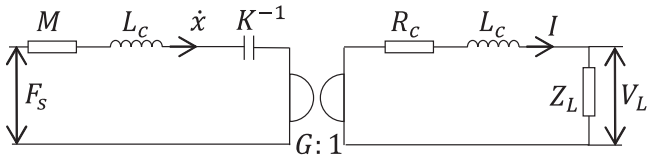

Figure 26. Equivalent circuit for a typical magnetostrictive system.

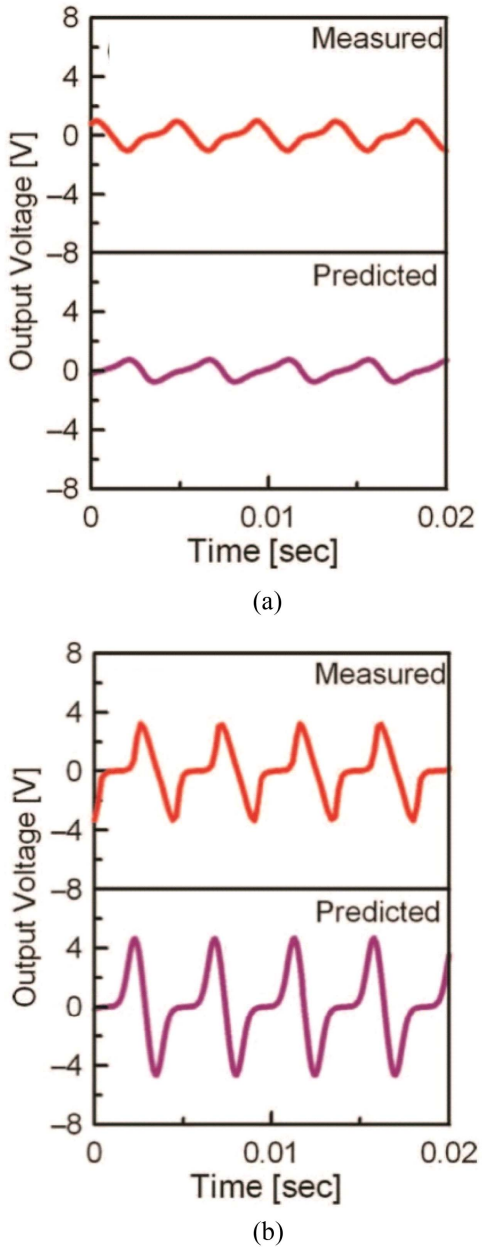

Figure 27. A comparison of modeled and measured output voltage from the Galfenol-based unimorph harvester developed by Yoo and Flatau under a 222 Hz sinusoidal base excitation: (a) the amplitude of base excitation is 9.8 m s^{-2} and (b) the amplitude of base excitation is 29.4 m s^{-2} [23].

where **A** is the vector magnetic potential, **H** is the magnetic field tensor, $\mathbf{J}_s$ is the current density tensor, σ is the electrical conductivity, and **n** is the normal direction of the boundary

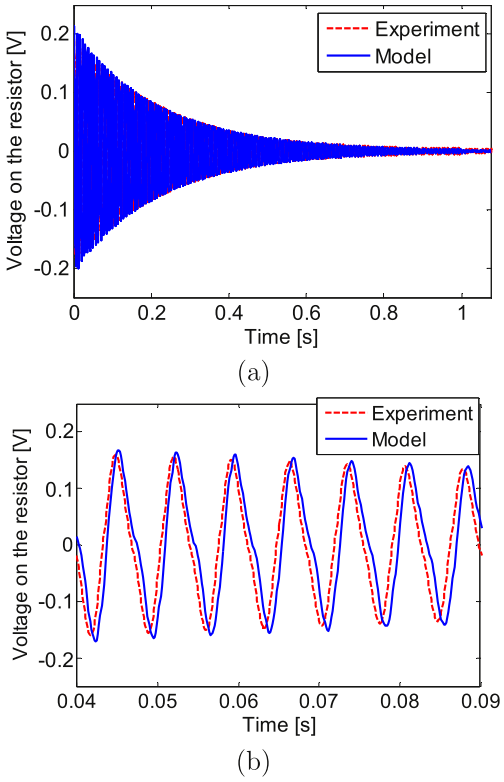

Figure 28. The measured and modeled output voltage of the unimorph harvester shown in figure 17(c) under 2 N impulsive tip excitation, when a 74 Ω and a 1 μF are attached to the pickup coil in parallel. (a) Impulsive response of the output voltage and (b) zoomed in view of the output voltage (0.04–0.09 s) [25].

surface ∂V_I. The electrical dynamics is described by a lumped parameter

$$V_o = Z(\mathbf{H}, \mathbf{T})I, \tag{23}$$

where $Z(\cdot,\cdot)$ denotes the field- and stress-dependent electrical impedance, I is the induced current, and V_o is the open-circuit voltage across the pickup coil.

Active magnetostrictive materials as well as passive surrounding components, which are described by (21) and (22), have been modeled using the FE method. Fully nonlinear magneto–mechanical coupling represented by a discrete energy averaged model [68] or an empirical constitutive model has been incorporated with the multiphysics FE framework [76–78, 80]. However, those models require large number of iterations and thus are time-consuming. Rezaeealam *et al* [79] simplified the FE framework by implementing lookup tables to describe the nonlinear magneto–mechanical coupling. Deng and Dapino [25] later utilized the discrete energy averaged model to generate lookup tables and presented a systematic optimization procedure for Galfenol-based unimorph harvesters. Deng and Dapino [25] recently incorporated electrical dynamics in (23) with the FE framework and accurately captured the influence of electrical impedance. Figure 28 presents the impulsive response of the unimorph energy harvester shown in figure 17(c) when a capacitive–resistive load is attached to the pickup coil.

7. Concluding remarks

Energy harvesters that scavenge usable energy from ambient vibration sources are able to provide sustainable power to wireless or wearable devices. This review investigated the recent technological advances on magnetostrictive vibration energy harvesters, especially those based on Terfenol-D and Galfenol. Compared with existing passive vibration energy harvesters (e.g. magnetoelectric or electromagnetic), magnetostrictive devices provide higher energy density. Compared with piezoelectric devices, magnetostrictive devices can generate similar levels of output power with no needs of power management circuit. Certain ductile and flexible magnetostrictive materials, such as Galfenol, Metglas, Alfenol, and C-Galfenol, are versatile in practice and can be integrated into MEMS. Thus, future research should focus on these mechanically-robust magnetostrictive materials.

This article categorized existing magnetostrictive vibration energy harvesters into the axial type and the bending type, based on the stress state in the magnetostrictive element. The axial type vibration energy harvesters require large excitation force and thus have to be mounted in load paths. These devices are able to generate a PD up to a level of $10\,\mathrm{W\,cm^{-3}}$, but complicated protection mechanisms are needed to protect certain magnetostrictive materials, such as Terfenol-D, from damage. The bending type devices, on the other hand, can be mounted on any vibrating surfaces. Their typical output PD is in a level of $10\,\mathrm{mW\,cm^{-3}}$. The bending type energy harvesters have been developed following three approaches: a single-layer magnetostrictive beam, a double-layer magnetostrictive beam (bimorph), and a magnetostrictive composite beam (unimorph). The output power from the single-layer magnetostrictive beam configuration is extremely small; the bimorph configuration also exhibits relatively small output power due to the dominant shear stresses. The unimorph configuration provides the maximum output power capability and requires more investigation.

Pickup coils, which create a mass penalty, are necessary to convert magnetic energy to electrical energy in magnetostrictive vibration energy harvesters. Previous studies have preliminarily investigated two possible solutions to eliminate bulky coils. The first solution is to manufacture magnetostrictive/piezoelectric composites, also known as magnetoelectric materials. However, drawbacks associated with piezoelectric energy harvesters, such as aging and high output impedance, exist in these devices. The other solution is to integrate magnetostrictive materials into MEMS. Micro-scale copper coils have been created around deposited Galfenol on top of Si and SiO_2 [81–83]. Potential achievements need to be further exploited following this path.

Another limitation associated with the magnetostrictive harvesters is that the device generates usable output power only near system resonances. The frequency bandwidth of a Galfenol-based unimorph harvester has been improved by 16% in experiments by driving a pre-buckled beam in a bistable state. Future studies should further explore bandwidth enhancement strategies by combining nonlinear instability with magnetostrictive systems.

Due to the lack of a universal performance metric for magnetostrictive vibration energy harvesters, comparison between different harvester devices is not straightforward. This review proposed, summarized, and compared several performance metrics and the performance of existing energy harvesters is compared following the proposed performance metrics.

The performance of magnetostrictive vibration harvesters highly depends on magnetic circuit design and electrical circuit design [84]. Recent achievements on magnetostrictive energy harvester modeling, including material-level modeling, lumped parameter models, and finite element models, are summarized. These efficient and accurate numerical models provide powerful tools for future magnetostrictive energy harvester development.

Acknowledgments

We wish to acknowledge the member organizations of the Smart Vehicle Concepts Center, a National Science Foundation Industry/University Cooperative Research Center (http://SmartVehicleCenter.org) established under NSF Grant IIP-1238286.

ORCID iDs

Zhangxian Deng https://orcid.org/0000-0003-1084-1738
Marcelo J Dapino https://orcid.org/0000-0003-4888-1903

References

[1] Chandrakasan A, Amirtharajah R, Goodman J and Rabiner W 1998 Trends in low power digital signal processing *Circuits and Systems, 1998. ISCAS'98. Proc. 1998 IEEE Int. Symp. on* vol 4, pp 604–7
[2] Mohri K 1984 Review on recent advances in the field of amorphous-metal sensors and transducers *IEEE Trans. Magn.* **20** 942–7
[3] http://newport.com/t/introduction-to-solar-radiation
[4] Martin A G, Emery K, Hishikawa Y, Warta W and Ewan D D 2015 Solar cell efficiency tables (version 45) *Prog. Photovolt., Res. Appl.* **23** 1–9
[5] http://hi-z.com
[6] Le T, Mayaram K and Fiez T 2008 Efficient far-field radio frequency energy harvesting for passively powered sensor networks *IEEE J. Solid-State Circuits* **43** 1287–302
[7] Hata M 1980 Empirical formula for propagation loss in land mobile radio services *IEEE Trans. Veh. Technol.* **29** 317–25
[8] Roundy S, Wright P K and Rabaey J 2003 A study of low level vibrations as a power source for wireless sensor nodes *Comput. Commun.* **26** 1131–44
[9] Scheidler J J and Asnani V M 2016 A review of noise and vibration control technologies for rotorcraft transmissions *Proc. Internoise (Hamburg, Germany)*
[10] Exner W 1995 NVH phenomena in light truck drivelines *SAE Technical Paper* 952641 (https://doi.org/10.4271/952641)
[11] El-Hami M, Glynne-Jones P, White N W, Hill M, Beeby S, James E, Brown A D and Ross J N 2001 Design and fabrication of a new vibration-based electromechanical power generator *Sensors Actuators* A **92** 335–42

[12] Glynne-Jones P, Tudor M J, Beeby S P and White N W 2004 An electromagnetic, vibration-powered generator for intelligent sensor systems *Sensors Actuators* A **110** 344–9

[13] Despesse G, Jager T, Jean-Jacques C, Léger J, Vassilev A, Basrour S and Charlot B 2005 Fabrication and characterization of high damping electrostatic micro devices for vibration energy scavenging *Proc. Design, Test, Integration and Packaging of MEMS and MOEMS* pp 386–90

[14] Meninger S, Mur-Miranda J O, Amirtharajah R, Chandrakasan A P and Lang J H 2001 Vibration-to-electric energy conversion *IEEE Trans. Very Large Scale Integr. (VLSI) Syst.* **9** 64–76

[15] Mitcheson P D, Green T C, Yeatman E M and Holmes A S 2004 Architectures for vibration-driven micropower generators *J. Microelectromech. Syst.* **13** 429–40

[16] Moss S, Barry A, Powlesland I, Galea S and Carman G P 2011 A broadband vibro-impacting power harvester with symmetrical piezoelectric bimorph-stops *Smart Mater. Struct.* **20** 045013

[17] Anton S R and Sodano H A 2007 A review of power harvesting using piezoelectric materials (2003–2006) *Smart Mater. Struct.* **16** R1

[18] Mitcheson P D, Yeatman E M, Rao G K, Holmes A S and Green T C 2008 Energy harvesting from human and machine motion for wireless electronic devices *Proc. IEEE* **96** 1457–86

[19] Wang L and Yuan F G 2008 Vibration energy harvesting by magnetostrictive material *Smart Mater. Struct.* **17** 045009

[20] Stoner E C and Wohlfarth E P 1948 A mechanism of magnetic hysteresis in heterogeneous alloys *Phil. Trans. R. Soc.* A **240** 599–642

[21] Ueno T and Yamada S 2011 Performance of energy harvester using iron-gallium alloy in free vibration *IEEE Trans. Magn.* **47** 2407–9

[22] Asnani V M, Deng Z, Scheidler J J and Dapino M J 2016 Experimental comparison of piezoelectric and magnetostrictive shunt dampers *Proc. SPIE* **9801** 98010R

[23] Yoo J and Flatau A B 2012 A bending-mode Galfenol electric power harvester *J. Intell. Mater. Syst. Struct.* **23** 647–54

[24] Deng Z and Dapino M J 2015 Modeling and design of Galfenol unimorph energy harvesters *Smart Mater. Struct.* **24** 125019

[25] Deng Z and Dapino M J 2016 Influence of electrical impedance and mechanical bistability on Galfenol-based unimorph harvesters *J. Intell. Mater. Syst. Struct.* **28** 421–31

[26] Roundy S 2005 On the effectiveness of vibration-based energy harvesting *J. Intell. Mater. Syst. Struct.* **16** 809–23

[27] Viktor B 2013 Vibration energy harvesting using Galfenol-based transducer *Proc. SPIE* **8688** 86881F

[28] Deng Z 2015 Nonlinear modeling and characterization of the villari effect and model-guided development of magnetostrictive energy harvesters and dampers *PhD Dissertation* The Ohio State University

[29] Deng Z and Dapino M 2017 Magnetic flux biasing of magnetostrictive sensors *Smart Mater. Struct.* **26** 055027

[30] Zhang H 2011 Power generation transducer from magnetostrictive materials *Appl. Phys. Lett.* **98** 2505

[31] Viola A, Franzitta V, Cipriani G, Dio V, Raimondi F M and Trapanese M 2015 A magnetostrictive electric power generator for energy harvesting from traffic: design and experimental verification *IEEE Trans. Magn.* **51** 1–4

[32] Liu H, Wang S, Zhang Y and Wang W 2014 Study on the giant magnetostrictive vibration-power generation method for battery-less tire pressure monitoring system *Proc. Inst. Mech. Eng.* C **229** 1639–51

[33] Yan B, Zhang C, Li L, Zhang H and Deng S 2015 Design and construction of magnetostrictive energy harvester for power generating floor systems *Electrical Machines and Systems (ICEMS), 2015 18th Int. Conf. on* pp 409–12

[34] Yan B, Zhang C and Li L 2015 Design and fabrication of a high-efficiency magnetostrictive energy harvester for high-impact vibration systems *IEEE Trans. Magn.* **51** 1–4

[35] Nair B, Nachlas J A and Murphree A 2014 Magnetostrictive devices and systems *US Patent App.* 14/181,574

[36] Murphree Z 2013 Magnetostrictive wave energy harvester with heave plate *US Patent App.* 13/928,035

[37] Dudley J H and Nachlas J A Vibration energy harvester, March 20 2014 *US Patent App.* 14/221,166

[38] Staley M E and Flatau A B 2005 Characterization of energy harvesting potential of Terfenol-D and Galfenol *Proc. SPIE* **5764** 630–40

[39] Staley M E 2005 Development of a prototype magnetostrictive energy harvesting device *PhD Dissertation* University of Maryland

[40] Scheidler J J and Dapino M J 2016 Mechanically induced magnetic diffusion in cylindrical magnetoelastic materials *J. Magn. Magn. Mater.* **397** 233–9

[41] Berbyuk V and Sodhani J 2008 Towards modelling and design of magnetostrictive electric generators *Comput. Struct.* **86** 307–13

[42] Park Y, Kang H and Wereley N M 2014 Conceptual design of rotary magnetostrictive energy harvester *J. Appl. Phys.* **115** 17E713

[43] Zucca M, Bottauscio O, Beatrice C, Hadadian A, Fiorillo F and Martino L 2014 A study on energy harvesting by amorphous strips *IEEE Trans. Magn.* **50** 1–4

[44] Kita S, Ueno T and Yamada S 2015 Improvement of force factor of magnetostrictive vibration power generator for high efficiency *J. Appl. Phys.* **117** 17B508

[45] Ueno T 2015 Performance of improved magnetostrictive vibrational power generator, simple and high power output for practical applications *J. Appl. Phys.* **117** 17A740

[46] Deng Z and Dapino M J 2015 Multiphysics modeling and design of Galfenol-based unimorph harvesters *Proc. SPIE* **9433** 94330B

[47] Adly A, Davino D, Giustiniani A and Visone C 2010 Experimental tests of a magnetostrictive energy harvesting device toward its modeling *J. Appl. Phys.* **107** 09A935

[48] Hu J, Xu F, Huang A and Yuan F 2011 Optimal design of a vibration-based energy harvester using magnetostrictive material (MsM) *Smart Mater. Struct.* **20** 015021

[49] Ueno T 2016 U-shape magnetostrictive vibration based power generator for universal use *Proc. SPIE* **9806** 98060E

[50] Li P, Wen Y, Liu P, Li X and Jia C 2010 A magnetoelectric energy harvester and management circuit for wireless sensor network *Sensors Actuators* A **157** 100–6

[51] Li M, Wen Y, Li P, Yang J and Dai X 2011 A rotation energy harvester employing cantilever beam and magnetostrictive/piezoelectric laminate transducer *Sensors Actuators* A **166** 102–10

[52] Wang Y, Gray D, Berry D, Gao J, Li M, Li J and Viehland D 2011 An extremely low eqluivalent magnetic noise magnetoelectric sensor *Adv. Mater.* **23** 4111–4

[53] Dai X, Wen Y, Li P, Yang J and Li M 2011 Energy harvesting from mechanical vibrations using multiple magnetostrictive/piezoelectric composite transducers *Sensors Actuators* A **166** 94–101

[54] Marin A and Priya S Multimodal vibration harvester combining inductive and magnetostrictive mechanisms, August 1 2013 *US Patent App.* 13/757,076

[55] Mori K, Horibe T, Ishikawa S, Shindo Y and Narita F 2015 Characteristics of vibration energy harvesting using giant magnetostrictive cantilevers with resonant tuning *Smart Mater. Struct.* **24** 125032

[56] Tsutsumi E, del Rosario Z and Lee C 2012 Vibration energy harvesting using the nonlinear oscillations of a magnetostrictive material *Proc. SPIE* **8341** 834104
[57] Moon F C and Holmes P J 1979 A magnetoelastic strange attractor *J. Sound Vib.* **65** 275–96
[58] Ferrari M, Ferrari V, Guizzetti M, Andò B, Baglio S and Trigona C 2010 Improved energy harvesting from wideband vibrations by nonlinear piezoelectric converters *Sensors Actuators* A **162** 425–31
[59] Erturk A and Inman D J 2011 Broadband piezoelectric power generation on high-energy orbits of the bistable duffing oscillator with electromechanical coupling *J. Sound Vib.* **330** 2339–53
[60] Van Blarigan L, Danzl P and Moehlis J 2012 A broadband vibrational energy harvester *Appl. Phys. Lett.* **100** 253904
[61] Mayergoyz I D 1991 *The Classical Preisach Model of Hysteresis* (Berlin: Springer)
[62] Al Janaideh M, Rakheja S and Su C 2009 A generalized Prandtl–Ishlinskii model for characterizing the hysteresis and saturation nonlinearities of smart actuators *Smart Mater. Struct.* **18** 045001
[63] Jiles D C and Atherton D L 1986 Theory of ferromagnetic hysteresis *J. Magn. Magn. Mater.* **61** 48–60
[64] Restorff J B, Wun-Fogle M, Clark A E and Hathaway K B 2006 Induced magnetic anisotropy in stress-annealed Galfenol alloys *IEEE Trans. Magn.* **42** 3087–9
[65] Atulasimha J, Akhras G and Flatau A B 2008 Comprehensive three dimensional hysteretic magnetomechanical model and its validation with experimental ⟨110⟩ single-crystal iron-gallium behavior *J. Appl. Phys.* **103** 07B336
[66] Armstrong W D 2003 An incremental theory of magneto-elastic hysteresis in pseudo-cubic ferro-magnetostrictive alloys *J. Magn. Magn. Mater.* **263** 208–18
[67] Deng Z, Scheidler J J, Asnani V M and Dapino M J 2016 Quasi-static major and minor strain-stress loops in textured polycrystalline $Fe_{81.6}Ga_{18.4}$ Galfenol *J. Appl. Phys.* **120** 243901
[68] Evans P G and Dapino M J 2010 Efficient magnetic hysteresis model for field and stress application in magnetostrictive Galfenol *J. Appl. Phys.* **107** 063906
[69] Zhao X and Lord D G 2006 Application of the Villari effect to electric power harvesting *J. Appl. Phys.* **99** 08M703
[70] Clemente C, Mahgoub A, Davino D and Visone C 2016 Multiphysics circuit of a magnetostrictive energy harvesting device *J. Intell. Mater. Syst. Struct.* (https://doi.org/10.1177/1045389x16685444)
[71] Scheidler J J and Dapino M J 2013 Nonlinear dynamic modeling and resonance tuning of Galfenol vibration absorbers *Smart Mater. Struct.* **22** 085015
[72] Scheidler J J and Dapino M J 2014 Stiffness tuning of FeGa structures manufactured by ultrasonic additive manufacturing *Proc. SPIE* **9059** 905907
[73] Cao S, Zhang P, Zheng J, Zhao Z and Wang B 2015 Dynamic nonlinear model with eddy current effect for stress-driven Galfenol energy harvester *IEEE Trans. Magn.* **51** 1–4
[74] Cao S, Zheng J, Guo Y, Li Q, Sang J, Wang B and Yan R 2015 Dynamic characteristics of Galfenol cantilever energy harvester *IEEE Trans. Magn.* **51** 1–4
[75] Scheidler J J and Asnani V M 2017 Validated linear dynamic model of electrically-shunted magnetostrictive transducers with application to structural vibration control *Smart Mater. Struct.* **26** 035057
[76] Shu L, Dapino M J, Evans P G, Chen D and Lu Q 2011 Optimization and dynamic modeling of Galfenol unimorphs *J. Intell. Mater. Syst. Struct.* **22** 781–93
[77] Chakrabarti S and Dapino M J 2010 A dynamic model for a displacement amplified magnetostrictive driver for active mounts *Smart Mater. Struct.* **19** 055009
[78] Deng Z and Dapino M J 2014 Characterization and finite element modeling of Galfenol minor flux density loops *J. Intell. Mater. Syst. Struct.* **26** 47–55
[79] Rezaeealam B, Ueno T and Yamada S 2012 Finite element analysis of Galfenol unimorph vibration energy harvester *IEEE Trans. Magn.* **48** 3977–80
[80] Davino D, Giustiniani A, Visone A and Zamboni W 2012 Stress-induced eddy currents in magnetostrictive energy harvesting device *IEEE Trans. Magn.* **48** 18–25
[81] Torii Y, Wakiwaka H, Kiyomiya T, Matsuo Y, Yamada Y and Makimura M 2005 Tb-Fe-Co giant magnetostrictive thin film and its application to force sensor *J. Magn. Magn. Mater.* **290** 861–4
[82] Wenzel C, Adolphi B, Merkel U, Jahn A, Marschner U, Ziske J, Neubert H and Fischer W 2009 Resonant bending sensor based on sputtered Galfenol *Sensors Actuators* A **156** 129–33
[83] Sauer S, Marschner U, Adolphi B, Clasbrummel B and Fischer W 2012 Passive wireless resonant Galfenol sensor for osteosynthesis plate bending measurement *IEEE Sens. J.* **12** 1226–33
[84] Cavaroc P, Curtis C, Naik S and Cooper J 2014 Single stage AC–DC converter for Galfenol-based micro-power energy harvesters *Proc. SPIE* **9115** 91150S